Annals of Agrarian Science

Journal homepage: http://journals.org.ge/index.php

Structural and Magnetic Properties of Silver Oleic Acid Multifunctional Nanohybrids

S. Khutsishvili[a], P. Toidze[b], M. Donadze[b], M. Gabrichidze[b*], T. Agladze[b], N. Makhaldiani[b]

[a]A.E. Favorsky Irkutsk Institute of Chemistry of the Siberian Branch of the Russian Academy of Sciences, 1, Favorskogo Str., Irkutsk, 664033, Russia

[b]Technical University of Georgia, Department of Chemical and Biological Technologies 69, M. Kostava Str., Tbilisi, 0175, Georgia

Received: 15 May 2018; accepted: 19 September 2018

ABSTRACT

Sols of core-shell silver NPs are synthesized by electrochemical method. The method provides the ability to adjust the particle size by changing both the concentration of oleic acid and the residence time τ_0 in the organic phase. We synthesized silver nanoparticles with oleic acid concentration of 0.25% (Ag&0.25%OA) and 0.75% (Ag&0.75%OA). These silver nanoparticles have been studied using modern physical–chemical methods: Transmission Electron Microscopy (TEM); Fourier Transform Infrared Spectroscopy (FT-IR); Dynamic Light Scattering (DLS); Thermogravimetric and Differential Thermal Analysis (TGA and DTA); Electron Paramagnetic Resonance (EPR). DTA curves indicate the chemical nature of bond ligand in the secondary shell.This conclusion supported by quantum chemical simulation by using quantum-chemical software HyperChem-8 and semi-empirical calculation method ZINDO. In the EPR spectra of silver-containing sols Ag&0.25%OA and Ag&0.75%OA a complex wide asymmetric signal with several resonant lines is recorded, which is consistent with a wide size distribution of nanoparticles. It is important to note that a change in the oleic acid layers of the nanoparticles seems to affect the dimension of the nanocrystallites that are being formed. The presence of the FMR resonance line in Ag&0.75%OA may indicates the presence of Ag-cubic cells in nanoparticles with internal magnetic fields significantly larger than the Zeeman field, the available EPR in the X-band range.

Keywords: Core-shell, Nanoparticles, Oleic acid, Ligand, Charge, Activation energy.

*Corresponding author: Maia Gabrichidze: E-mail address: gabrichidze.maia@gmail.com

Introduction

Silver nanoparticles is one of the important and interesting nanomaterials, the use of which is promising in the environment (water and air purification, catalysis), in the field of biomedicine (diagnosis and treatment of cancer), food industry (packaging materials), in the manufacture of medical instruments (antibacterial coatings), in optical devices, cosmetics, in the pharmaceutical industry.

Due to their nano-size, metallic silver particles have unique physicochemical, biological properties that are associated with an increased ratio of surface area to volume. In this regard, it is necessary to determine the physicochemical properties of nanoparticles in order to establish the expected chemical, physical and catalytic activity.

Effective application of nanoparticles as building blocks in bottom-up design of multicomponent nano-composites requires monitoring of fundamental properties, such as size, charge, chemical reactivity and ability of nanoparticles to disperse in various media. Owing to high aspect ratio, metal nanoparticles tend to agglomeration, aggregation and corrosion processes finally leading to loss of valuable properties inherent to building of blocks. Chemisorption of organic ligand shell

provides steric stabilization of nanoparticle core preventing its degradation. The present study is focused on characterization of metal core-ligand shell interactions as well as on ligands molecules interaction in primary and secondary layers of the shell - phenomena largely determining bottom-up strategy for synthesis of multifunctional hybrid nanoparticles [1].

Experimental

Chemicals and instruments. The reagents used in this study are purchased from Sigma-Aldrich unless otherwise specified and used without purification. Chemical interactions of surfactant with NPs studied by FT-IR spectroscopy in a range of 400–4000 cm^{-1} with the resolution of 0.5 cm^{-1} (Thermo Nicolet, Avatar 370) use the KBr technique. Size, shape and chemical composition of isolated NPs are estimated from TEM (Tesla BS 500) and SEM (JSM-6510LV) images. The samples are prepared by placing small drops of a sol onto the carbon-coated copper grid. The size distribution of NPs in a sole is evaluated from laser beam dynamic light scattering data (Zetasizer-Nano, Malvern). Prior to sample placing into a cuvette, the as-prepared sols are diluted with hexane 1:8. The structural and thermal stability properties of nanoparticles are characterized by thermo-gravimetric analysis (TGA) and differential thermal analysis (DTA) technique (NETZSCH, STA-2500, Regulus). In both cases characterized by activation energies calculated from OA transformation during the thermal decomposition, using Ozawa -Flynn-Wall method derived from the integral iso-conversional method [2, 3].

EPR spectra were recorded on a FT X-band Brüker ELEXSYS E-580 spectrometer (X-wave range 9.7 GHz). Precision of the measurement of *g*-factor was ±0.00018. CW EPR-spectra were recorded of the 1 and 3 samples (0.025 g) at the following conditions: amplitude modulation 10.0 G, modulation frequency 100 kHz, averaged scans 35, field range 3000 G / centre field 3100 G, time constant 0.04 s, conversion time 0.12 s, microwave power 0.6325 mW. CW EPR-spectra were recorded of the 4 and 5 samples (0.025 g) at the following conditions: amplitude modulation 10.0 G, modulation frequency 100 kHz, averaged scans 1, field range 6800 G / centre field 3500 G, time constant 0.04 s, conversion time 0.12 s, microwave power 0.6325 mW.

The metals percentage of the studied nanocomposites was evaluated by atomic absorption analysis using a HITACHI TM 3000, detector SDD XFlash 430-H (Table 1).

Preparation of sols of AgNPs. Sols of silver NPs in a hexane are synthesized by electrochemical method in a reactor consisting of sacrificial silver anode (99.9% purity), and aluminum (99.9%) cathode, which upon rotation crosses immiscible layers of aqueous (0.05 M $AgNO_3$, doubled distilled water) and organic (hexane, 0. 25% and 0. 75% OA) solvents [1, 4]. The experimental set-up allows silver ions formed at the anode to discharge at the cathode surface poisoned by surfactant (OA), which adsorbs at sites favorable for silver adatoms and inhibits the growth of silver nanoclusters. The latter is weakly adsorbed at the surface and strongly bonded to amphiphile OA molecules which are easily washed out from cathode upon rotation forming stable sols of Ag–OA core–shell NPs in hexane. The method provides the ability to adjust the particle size by changing both the concentration of oleic acid and the residence time τ_0 during which the metal cluster formed at the border of the cathode-water electrolyte allows the amphiphile surfactants to adsorb from the organic phase. The results of measuring the size of silver nanoparticles using the DLS method are shown (Table 2).

Table 1. *The elemental analysis of the samples*

Sample	Mass content, %		
	C	O	Ag
Ag&0.25%OA	11.8	3.6	84.6
Ag&0.75%OA	12.8	3.9	83.3

Table.2. *Size of silver nanoparticles coverage by oleic acid*

Concentration OA(%)	Z-Average (d.nm)	PdI	τ_o (sec)
0.25	15.62	0.15	45
0.50	14.95	0.14	42
0.75	15.74	0.14	39
1.00	16.96	0.24	36

In the present study, electrosynthesis has been carried out at experimental conditions yielding assembles of spherical silver NPs Ag&0.25%OA by TEM (Fig. 1a). The histogram (Fig. 1b) of the size distribution shows the average diameter of the NPs is 14.4±4.2nm. ΔQ – number of particles in %. Size distribution of Ag&0.25%OA and Ag&0.75%OA determined from DLS method is Z_{ave}=15.62 nm, PdI= 0.15 and Z_{ave}=15.74 nm, PdI= 0.14 (Table 2).

FT-IR spectroscopy. The chemical bonding of OA molecules to silver nanoclusters in diluted OA solutions are characterized by appearance of two new bounds at 1639 and 1509 cm^{-1} (Fig. 2a) which are typical for the asymmetric and symmetric carboxylate stretch. These effects are interpreted as the evidence of OA bidentate bonding to silver via two symmetrically coordinate oxygen atoms of the carboxylate head [5]. The effect of increase in oleic acid concentration on FT-IR spectra characteristics (Fig.2b). According to these data the major effect is appearance of a new peak at 1708.6cm^{-1} that is characteristic for C=O bond stretch.

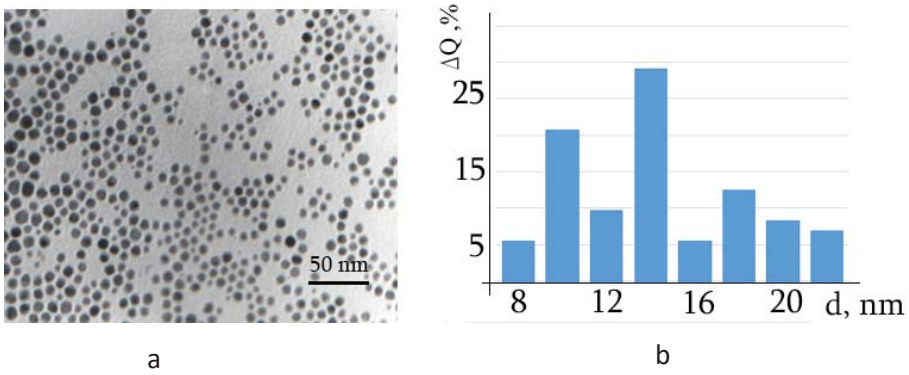

Fig. 1. *TEM image (a) and histogram of the size distribution (b) of silver NPs capped of 0.25%OA*

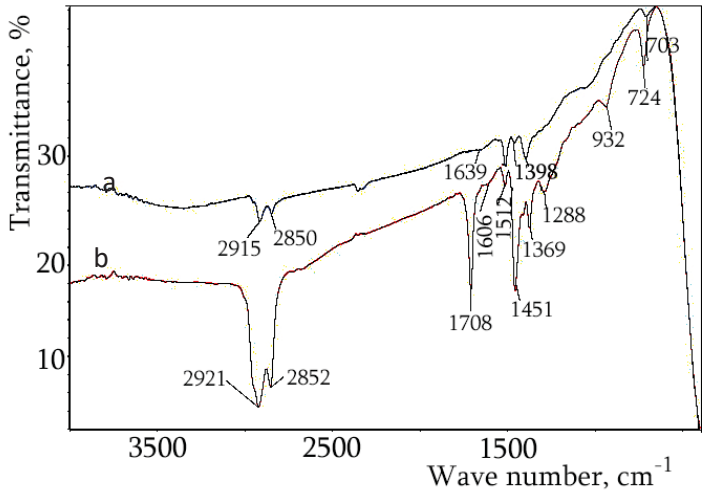

Fig. 2. *FT-IR spectra silver nanoparticles capped by monolayer (a) and bilayer (b)*

TGA and DTA measurements data. The application of dynamic TG methods holds great promise as a tool for unraveling the mechanisms of physical and chemical processes occurred during the decomposition of solids. In this investigation, Ozaw -Flynn-Wall- (OFW) methods have been used to analyze the non-isothermal desorption kinetics of silver nanoparticles capped with oleic acid ligand. TGA and DTA curves of Ag&0.25%OA and Ag&0.75%OA samples are measured at heating rate (β) 5 K/min (Fig. 3 a, b).

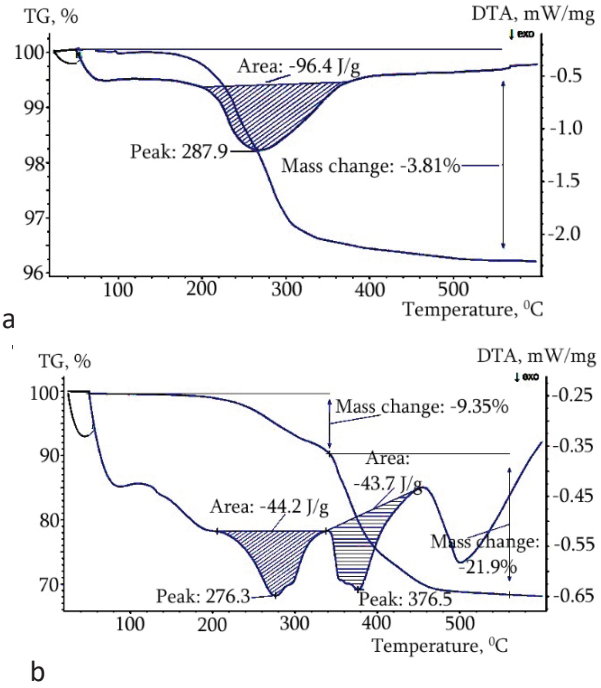

Fig. 3. *TGA and DTA curves of Ag&0.25% OA (a) and Ag&0.75% OA (b) samples*

TGA patterns in diluted OA solutions are characterized by one step mass loss (3.81%) curve. DTA curve measured under the same conditions displays exothermic peak at 287.9 °C. Corresponding enthalpy is 96.4 J/g. Contrary to these data, TGA curves measured in OA rich solutions display two step mass loss 9.35 % (50 – 340 °C) and 21.89 % (340-600 °C). Corresponding DTA curve displays two exothermic peaks at 276.3 and 376.5 °C. Calculated enthalpies are 44.22 J/g and 43.77 J/g. Thermodesorption E_a values have been calculated by Ozawa-Flynn-Wall (OFW) method derived from the integral iso-conversional method using Doyle's approximation (Equation 1) [6].

$$f(a) \approx 7.03 \cdot 10^{-3} \cdot \frac{AE_a}{\beta R} \exp(-1.052 E_a / RT) \quad (1)$$

According to this method:

$$\ln \beta = \ln \frac{AE_a}{Rg(x)} - 5.331 - 1.052 \cdot \frac{E_a}{RT} \quad (2)$$

where A is frequency factor and g (x) is function depends on the rate of conversion, β – heating rate, T – temperature, R = 8.31J/mol·K. Thermodesorption activation energies calculated by OFW method (Equation 1) as a function of the conversion degree (Fig. 4). Sharp increase in E_a observed at low mass losses in concentrated solution indicates the change of desorption mechanism in bilayer system.

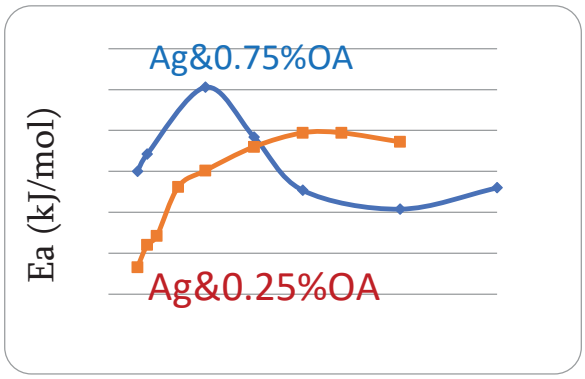

Fig. 4. *Thermodesorption activation energies calculated by OFW method as a function of the conversion degree.*

The calculation of the coating of nanoparticles with OA was calculated according to equation 3.

$$N = \frac{4\rho r^3 \pi \omega N_A}{3(100-\omega)M_{OA}} \quad (3)$$

where N is the number of oleic acid ligands per particle, ρ = 10.49g/cm^3 is the density of the silver, r= 7.2nm is the average radius of the Ag&0.25%OA (based on the TEM results, Fig.1), ω=3.81% is the weight loss (in %), N_A = 6.022 × 10^{23} mol^{-1}, is Avogadro's constant, and M_{OA} = 282.47 g/mol is the molecular weight of oleic acid.

The number of ligands was calculated for Ag&0.25%OA N=1385. Assuming that the surface of the NPs is covered with a close packed monolayer of the surfactant, the surface area S occupied by the oleic acid ligand A indicates the ratio of the total surface area of the particle to the number of oleic acid ligands A=0.46nm^2. Considering the fact that the area of one molecule of oleic acid S=0.21nm^2, percentage of silver nanoparticle surface coating

with oleic acid molecules is 45%.

Quantum-chemical simulation. Molecular models of free and adsorbed oleic acid at silver NPs are created by using quantum-chemical software HyperChem-8 and semi-empirical calculation method ZINDO1[7]. Electrostatic potentials significantly vary from chemisorbed OA molecules (Fig.5 a,b). Ligand interaction with Ag NPs results in increase of effective charge and electrostatic potential at silver surface indicating charge transfer from ligand carboxyl group to nanoparticle atoms.

Formation of a secondary layer in solutions rich in OA is accompanied by increase electrostatic potential at silver.

According to quantum, chemical calculations of chemisorbed OA silver ligand interaction resulted in redistribution of electron density at OA molecule. The electrostatic potential at carboxyl group of monolayer and bilayer OA are U_1=-1.173e/Å and U_2=-1.217e/Å correspondingly (Fig.5a,b).

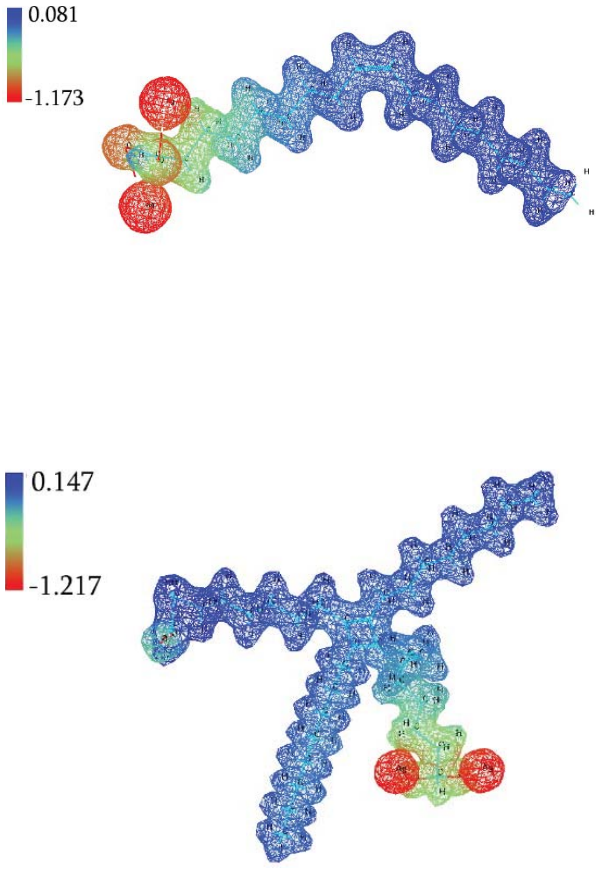

Fig. 5. *Electrostatic potentials maps for chemisorbed mono (a) and bilayer (b) OA molecules.*

Discussion

An increasing volume of studies aimed at examination of the mechanism of unsaturated fatty acid ligands interaction with metals and metal oxide cores have been conducted by means of TEM, DLS, FT-IR, TGA, DTA and EPR methods [8-16]. The bidentate covalent bonding of oxygen atoms of polar carboxylic groups with core NPs assumed to be the driving force formation of chemisorbed ligand monolayer. Appearance of a new FT-IR peak at 1708cm^{-1} characteristic for C=O bond stretch (Fig. 2b), as well as two step mass loss TGA curves and appearance two exothermic peaks at DTA curves (Fig.3b) shown in present study clearly demonstrate that at high OA concentration Ag NPs are capped by adsorbed ligand bilayers. Contrary to widely accepted concept on physical nature of ligands, bonding in the secondary shell [8, 9, 16] significant enthalpies calculated from DTA curves indicates the chemical nature of bonding. This conclusion supported by quantum chemical simulation leads to the model of formation C=C double bonds as a result of coupling of delocalized p-electrons of primary and secondary layers. Inversion of the secondary OA layer apparently originated from repulsion of polar carboxylic groups in a secondary shell owes to increase in negative charge at oxygen atoms. Finally, this leads to formation of branching ligand network. The other important conclusion on the mechanism of ligand chemisorption is followed from variation of thermodesorption activation energies with conversion degree (Fig.4). It is widely accepted that formation of ligand primary adsorbed layer follows Langmuir low, which assumes adsorption at homogenous substrate and predicts independence of adsorption energy from surface coverage. Our experimental data are in sharp disagreement with these assumptions. In contradiction to Langmuir adsorption model the data shown at Fig.4 testify a significant change in thermodesorption activation energy with variation in a number of adsorbed OA molecules in a primary shell. To interpret activation energy patterns we have to account for the fact that nanoparticles surface formed under highly nonequilibrium conditions due to artificial termination of crystal grow and freezing irregular structure by capping agent. These leads to more realistic model accounting for effect of surface inhomogeneity resulting in increase of adsorption energy with surface coverage. Complex variation of $E_{a.}$ with mass loss in presence of OA excess apparently

reflects contribution of several factors: increase in E_a as OA molecules desorbed from sites with higher adsorption energy and simultaneous variation in chemical bond strength in a secondary layer.

EPR. In the EPR spectra of silver-containing sols Ag&0.25%OA and AG&0.75%OA, a complex wide asymmetric signal with several resonant lines is recorded (Fig.6), which is consistent with a wide size distribution of nanoparticles [10-12]. In similar metal-containing nanosystems, like other disordered or partially ordered systems, have a spread in the symmetries of the nearest environment of individual paramagnetic centers, so in the EPR spectra we observe not one line, but the envelope of a set of lines with close, but different from each other parameters. The presence of nanoparticles of different diameters and different supramolecular organization of the system as a whole, including.

The inevitable absence of a regular periodic structure and the uneven distribution of nanoparticles in a stabilizing medium, affects the symmetry of the signal. The lines with a peak-to-peak width ΔH_{pp} of several hundred Gauss are caused by collective electronic spin phenomena for a metal-containing nanomaterial [13], which are explained as RKKY interactions, exchange interactions of magnetic ions with conduction electrons [14-17], significant line broadening can be attributed to Korringa interaction [16], ferromagnetism [13, 17] and other exchange interactions [18].

The EPR signal (1), the so-called superpara-magnetic, consists of several overlapping components with an average *g*-factor of 2.09-2.13 and a line width (ΔH) of about 500-800 G. This line is due to the conduction electrons of CESR nanoparticles [12, 13, 19, 20], while the spin-orbit interaction for bulk Ag is so significant that the resonant signal can be observed only at very low temperatures [21]. Such a broad signal can also be associated with some localized EPR active (paramagnetic) surface states. Note in the case Ag&0.25%OA sols with the one layer of oleic acid (Fig. 6a) in comparison with Ag&0.75%OA, the broad line becomes more intense with a changing environment due to decrease in the "shielding" of the nanoparticles between themselves. In addition, the nanoscale particles are closely located to each other, as a result of which dipole-dipole interactions between them intensify, which also could be leads to an additional line broadening.

In the EPR spectra of silver-containing sols, the anisotropic signal (2), which belongs to divalent silver. The appearance of such highly oxidized silver states on the surface of nanoparticles occurs through the disproportionation of Ag(I), which leads to the formation of Ag(II) ions and metal Ag^0 silver [22, 23]. EPR characteristics of the complexes accord with the available literature data for analogous two-valence silver [24, 25].

It is important to note that a change in the oleic acid layers of the nanoparticles seems to affect the dimension of the nanocrystallites that are being formed. Thus, in the sols, when passing from the mono- to the bilayer of oleic acid, both small particles and larger multidomain agglomerates are found. So, the narrow weak signal (3) in the region of the *g*-factor 2.005 also refers to the spin resonance of conduction electrons from zero-valent silver [24, 26-28]. This line is usually characteristic of small nanoparticles, usually around 2 nm [29-30]. The presence of the FMR resonance line (4) in Ag&0.75%OA may indicates the presence of Ag-cubic cells in nanoparticles with internal magnetic fields significantly larger than the Zeeman field, the available EPR in the X-band range (Fig. 6b) [10, 13, 17]. At low temperature of 77 K the FMR signal is broadened several times. This resonance line arises from silver nanocrystallites with the properties of a bulk material representing a multi-domain system, where spins are oriented along the direction of the field.

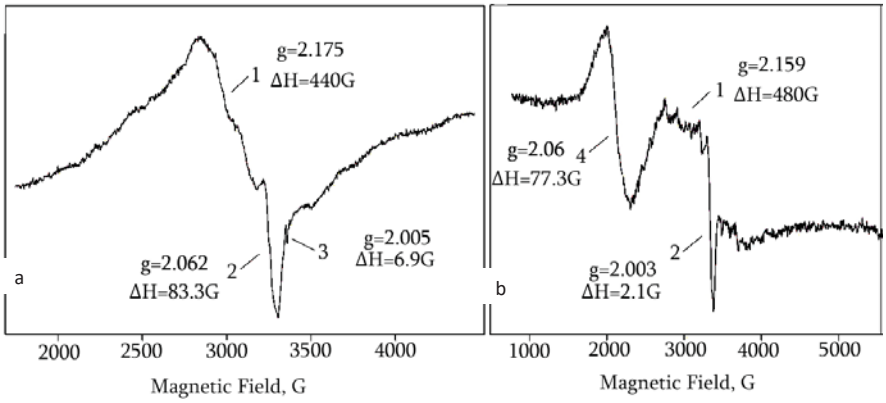

Fig. 6. *Ag&0.25% OA (a) and Ag&0.75% OA (b)*

The inevitable absence of a regular periodic structure and the uneven distribution of nanoparticles in a stabilizing medium, affects the symmetry of the signal. The lines with a peak-to-peak width ΔH_{pp} of several hundred Gauss are caused by collective electronic spin phenomena for a metal-containing nanomaterial [13], which are explained as RKKY interactions, exchange interactions of magnetic ions with conduction electrons [14-17], significant line broadening can be attributed to Korringa interaction [16], ferromagnetism [13, 17] and other exchange interactions [18].

The EPR signal (1), the so-called superparamagnetic, consists of several overlapping components with an average *g*-factor of 2.09-2.13 and a line width (ΔH) of about 500-800 G. This line is due to the conduction electrons of CESR nanoparticles [12, 13, 19, 20], while the spin-orbit interaction for bulk Ag is so significant that the resonant signal can be observed only at very low temperatures [21]. Such a broad signal can also be associated with some localized EPR active (paramagnetic) surface states. Note in the case Ag&0.25%OA sols with the one layer of oleic acid (Fig. 6a) in comparison with Ag&0.75%OA, the broad line becomes more intense with a changing environment due to decrease in the "shielding" of the nanoparticles between themselves. In addition, the nanoscale particles are closely located to each other, as a result of which dipole-dipole interactions between them intensify, which also could be leads to an additional line broadening.

In the EPR spectra of silver-containing sols, the anisotropic signal (2), which belongs to divalent silver. The appearance of such highly oxidized silver states on the surface of nanoparticles occurs through the disproportionation of Ag(I), which leads to the formation of Ag(II) ions and metal Ag^0 silver [22, 23]. EPR characteristics of the complexes accord with the available literature data for analogous two-valence silver [24, 25].

It is important to note that a change in the oleic acid layers of the nanoparticles seems to affect the dimension of the nanocrystallites that are being formed. Thus, in the sols, when passing from the mono- to the bilayer of oleic acid, both small particles and larger multidomain agglomerates are found. So, the narrow weak signal (3) in the region of the *g*-factor 2.005 also refers to the spin resonance of conduction electrons from zero-valent silver [24, 26-28]. This line is usually characteristic of small nanoparticles, usually around 2 nm [29-30]. The presence of the FMR resonance line (4) in Ag&0.75%OA may indicates the presence of Ag-cubic cells in nanoparticles with internal magnetic fields significantly larger than the Zeeman field, the available EPR in the X-band range (Fig. 6b) [10, 13, 17]. At low temperature of 77 K the FMR signal is broadened several times. This resonance line arises from silver nanocrystallites with the properties of a bulk material representing a multi-domain system, where spins are oriented along the direction of the field.

Conclusion

In the present study we claimed, that secondary ligand layer of the shell forms branching structure of chemically bonded ligand molecules. This conclusion supported by quantum chemical simulation which leads to the model of formation C=C double bonds resulting from coupling of delocalized p- electrons of primary and secondary layers. Desorption activation energy patterns displayed significant variation in activation energies with ligand surface coverage testifying inconsistence with widely accepted Langmuir adsorption model. More realistic model of ligand chemisorption accounting for energetic inhomogeneity of metal nanoparticle surface is proposed. In the EPR spectra of silver-containing sols Ag&0.25%OA and Ag&0.75%OA a complex wide asymmetric signal with several resonant lines is recorded, which is consistent with a wide size distribution of nanoparticles. It is important to note that a change in the oleic acid layers of the nanoparticles seems to affect the dimension of the nanocrystallites that are being formed. The presence of the FMR resonance line in Ag&0.75%OA may indicates the presence of Ag-cubic cells in nanoparticles with internal magnetic fields significantly larger than the Zeeman field, the available EPR in the X-band range.

Acknowledgments

The above project has been fulfilled with financial support of Shota Rustaveli National Science Foundation of Georgia (GrantNo.217020). Any idea in this publication is possessed by the author and may not represent the opinion of Shota Rustaveli National Science Foundation of Georgia.

The authors are grateful to the Baikal Analytical Center for the special measurements. Research completed by Khutsishvili Spartak in the framework

of the scientific project V.44.1.2. of the program of fundamental research of SB RAS.

References

[1] M. Donadze, M. Gabrichidze, S. Calvache, T. Agladze, Novel method of preparation of the hybrid metal (I) – metal (II) oxide nanoparticles, Int. J. Transactions of the IMF 94 (1) (2016)16-23.

[2] J.H. Flynn, The Isoconversional method for determination energy of activation at constant heating rate, J. Therm. Anal. 27 (1) (1983) 95-102.

[3] T. A. Ozawa New method of analyzing thermogravimetric data, Bull. Chem. Soc. Japan 38 (1965) 1881-1886.

[4] T. Agladze, M. Donadze, P. Toidze et al. Synthesis and Size Tuning of Metal Nanoparticles, Z.Phys. Chem. 227 (2013) 1187-1198.

[5] D.H. Lee FTIR spectral characterization of thin film coatings of oleic acid on glasses, J. Mat. Sci. 34 (1999) 139-146.

[6] C. Doyle, Kinetic analysis of thermogravimetric data, J. Appl. Polym. Sci. 5 (15) (1961) 285–292.

[7] K.Yang, H.Peng, Y.Wen, N. Li, Re-examination of characteristic FTIR spectrum of secondary layer in bilayer oleic acid-coated Fe_3O_4 nanoparticles, Appl. Surf. Sci. 256 (2010) 3093–3097.

[8] Q. Lan, C. Liu, F. Yang et al., Synthesis of bilayer oleic acid-coated Fe_3O_4 and interface nanoparticles and their application in pH-responsive Pickering emulsions, J. Coll. Sci. 310 (2007) 260–269.

[9] L. Shen, P.E. Laibinis and T.A. Hatton, Bilayer surfactant stabilized magnetic fluids: synthesis and interactions at interfaces, Langmuir 15 (1999) 447-453.

[10] S. Nellutla, S. Nori, S.R. Singamaneni, J.T. Prater, J. Narayan, A.I. Smirnov, Multi-frequency ferromagnetic resonance investigation of nickel nanocubes encapsulated in diamagnetic magnesium oxide matrix, J. Appl. Phys. 120 (22) (2016) 1-9.

[11] V. Angelov, H. Velichkova, E. Ivanov, R. Kotsilkova, M.H. Delville, M. Cangiotti, A. Fattori, M.F. Ottaviani, EPR and rheological study of hybrid interfaces in gold-clay- epoxy nanocomposites, Langmuir 30 (44) (2014) 13411-13421.

[12] M.V. Lesnichaya, B.G. Sukhov, E. Gasilova, G. Aleksandrova, T. Vakul'skaya, S. Khutsishvili, A. Sapozhnikov, I. Klimenkov, B. Trofimov, Chiroplasmonic magnetic gold nanocomposites produced by one-step aqueousmethod using κ-carrageenan, Carbohydrate Polymers 175 (2017) 18-26.

[13] A. Smirnov, EPR studies of nanomaterials. In: (Ed.) S. Misra, Multifrequency Willey-VCH, Verlag (2011) 825-843.

[14] M. Schlott , H. Schaeffer, B. Elschner, Gd^{3+}-ESR in the intermediate valent cerium compounds $Ce_xLa_{1-x}Os_2$, Zeitschrift für Physik B Condensed Matter 63 (4) (1986) 427- 436.

[15] J. Stöhr, H. Siegmann, Magnetism: From Fundamentals to Nanoscale Dynamics, Springer-Verlag, Berlin Heidelberg, 2006.

[16] P. Venegas, P. Netto, Exchange narrowing effects in the EPR linewidth of Gd diluted in Ce compounds, J. Appl. Phys. 83 (11) (1998) 6958-6968.

[17] P. Shin, S. Wu, Magnetic anisotropic energy gap and strain effect in Au nanoparticles, Nanoscale Research Letters 5 (2010) 25-30.

[18] M. Kakazey, N. Ivanova, G. Sokolsky, J. Gonzalez-Rodriguez, Electron paramagnetic resonance of MnO_2 powders, Electrochemical and Solid-State Letters 4 (5) (2001) 1-4.

[19] F. Blatter, K. Blazey, Conduction electron spin resonance of silver in zeolite AgY, Z. Phys. D - Atoms, Molecules and Clusters 18 (1991) 427-429.

[20] S. Sako Kimura, K. Size, Effect in CESR of magnesium and calcium small particles, Surface Sci. 156 (1985) 511-515.

[21] X. Li, A.Vannice, ESR studies of well-dispersed Ag crystallites on SiO_2, J. Catalysis 151 (1995) 87-95.

[22] M. Ali, A. Shames, S. Gangopadhyay, B. Saha, D. Meyerstein, Silver(II) complexes of tetrazamacrocycles: studies on e.p.r. and electron transfer kinetics with thiosulfate ion, Transition Metal Chemistry (Dordrecht, Neth.) 29 (2004) 463-470.

[23] M. Kester, A. Allred, Ligand-induced disproportionation of silver (I), J. American Chemical Society 94 (1972) 7189-7189.

[24] S. Khutsishvili, T. Vakul'skaya, N. Kuznetsova, T. Ermakova, A. Pozdnyakov, G. Prozorova, Formation of stable paramagnetic nano-compositescontaining zero-valence silver and copper in a polymeric matrix, J. Phys. Chem. C

118 (33) (2014) 19338–19344.
[25] J. McMilan, B. Smaler, Paramagnetic resonance of some silver(II) compounds. J. Chem. Phys. 35 (1961) 1698-1701.
[26] H. Moon, J. Kim, M. Suh, Redox-active porousorganic framework Chemie producing silver nanoparticles from AgI ions at room temperature, Angew.Chem. Int. Ed. 44 (2005) 1261-1265.
[27] G. Deligiannakis, Y. Trapalis, C. Boukos, N. Kordas, CW and pulsed EPR study of silver nanoparticles in SiO_2 matrix, J. Sol-Gel Science Technology 13 (1998) 503–508.
[28] S. Khutsishvili, T. Vakul'skaya, G. Aleksandrova, B. Sukhov, Stabilized silver nanoparticles and clusters Ag_n of humic-based bioactive nanocomposites, J. Cluster Sci. 28 (2017) 3067-3074.
[29] V. Timoshenko, T. Shabatina, Yu. Morozov, G. Sergeev, Complexation and chemical transformations in the ternary system silver-carbon tetrachloride- mesogenic cyanobiphenyl at low temperatures, J. Struc. Chem. 47 (1) (2006) 145-150.
[30] J. Michalik, H. Yamada, D. Brown, L. Kevan, Small silver clusters in smective clay interlayers, J. Phys. Chem. 100 (1996) 4213-4218.